X-Y-Y' Framework for Soil Consolidation

Prof. Sudhir K. Tewatia (Corresponding Author) CMD, Tewatia Edu-Globe, Jaipur, INDIA
Email: sdhirtewatia@gmail.com

Subject Categories: Civil Engineering (Geotechnical Engineering, Transportation Engineering)

Abstract

The stability of global civil infrastructure relies fundamentally on accurately predicting soil consolidation, a multi-dimensional dissipative process with time or pressure centric traditional models. This classical framework forces dynamic's three-dimensional phenomena into two-dimensional projections, inevitably triggering the "Missing Time" problem. When the exact initial loading time ($t=0$) is unknown—a common reality in forensic geotechnics and historical preservation—classical initial-value formulations fail, completely paralyzing dynamic analysis. This paper introduces the comprehensive 3D X-Y-Y' Calculus framework, originating from complex soil mechanics, which resolves this fundamental limitation. By establishing the observable state (Settlement) and instantaneous rate of settlement (Velocity) as the primary independent dimensions, Time (t) is transformed from a master variable into a dependent geometric consequence. The framework formalizes the Asymptotic Linearity Theorem (ALT) across a trinity of phases: Type I-III (Diffusion), Type IV (Creep), and Type V (Compression). It mathematically proves that multi-dimensional consolidation trajectories—including radial drainage, which linearizes as early as 5-10% consolidation—converge to invariant linear phase-space attractors. The Central Operator (Λ) is derived to extract hydrodynamic properties directly from geometric slopes, bypassing chronological initial conditions entirely. Graph-theoretic principles are introduced to model complex, multi-layered anisotropic strata. Validated on numerous soils through numerical examples and global infrastructure challenges—including the Leaning Tower of Pisa, Mexico City's subsidence, and the MOSE project—the X-Y-Y' calculus provides a universal paradigm for parameter extraction, predictive modelling, and stability diagnosis in systems where the clock has no zero. This is valid on 3D crack monitoring also that may be seen in sinking or equilibrium achieving civil engineering infrastructures.

Keywords: *Soil Consolidation, Settlement, Compression Index, Clay, Dynamic Systems, Sustainable Infrastructure, Mathematical Modelling, Geotechnical Engineering*

Summary

Consolidation is a core area of geotechnical engineering. The stability, resilience, and operational longevity of global civil infrastructure are fundamentally reliant on the accurate prediction of the consolidation settlement of the underlying geological strata. In both theoretical soil mechanics and applied field practice, soil consolidation manifests as a highly complex, multi-dimensional phenomenon characterized by the intricate intermixing of hydrodynamic fluid

diffusion and visco-plastic structural creep. Compounding this inherent complexity are the frequently unknown initial conditions of chronological time, effective pore pressure, and baseline settlement, alongside the realities of non-uniform structural loading, haphazard drainage boundaries, and highly anisotropic soil stratigraphy. Traditional geotechnical engineering relies almost exclusively on classical methods, which rigidly privilege chronological time (t) as the absolute independent variable and treat the settlement (δ), rate of settlement ($d\delta/dt$) merely as a derived, dependent property. This time-centric mathematical paradigm forces the three-dimensional dynamic reality of soil consolidation into incomplete two-dimensional projections, permanently obscuring the intrinsic geometric nature (δ-$d\delta/dt$) of the dissipative system (Fig 1-2).

A critical and highly destructive consequence of this dimensional reduction is the "Missing Time" problem—the absolute mathematical inability of classical initial-value formulations to accurately predict settlement trajectories, or to reconstruct historical deformation, when the exact initial start time of structural loading (t_0) is unknown or physically undefined. This limitation effectively paralyzes dynamic analysis in forensic geotechnics, historical preservation, and large-scale satellite infrastructure monitoring. In response, this paper details the formalization of the 3D X-Y-Y' Calculus framework. Originating from the rigorous study of complex soil consolidation behavior during the late 1990s, this framework completely inverts the classical paradigm by establishing the physically observable state (Settlement, δ) and the instantaneous rate (Velocity of Settlement, $d\delta/dt$) as the primary independent dimensions. By prioritizing

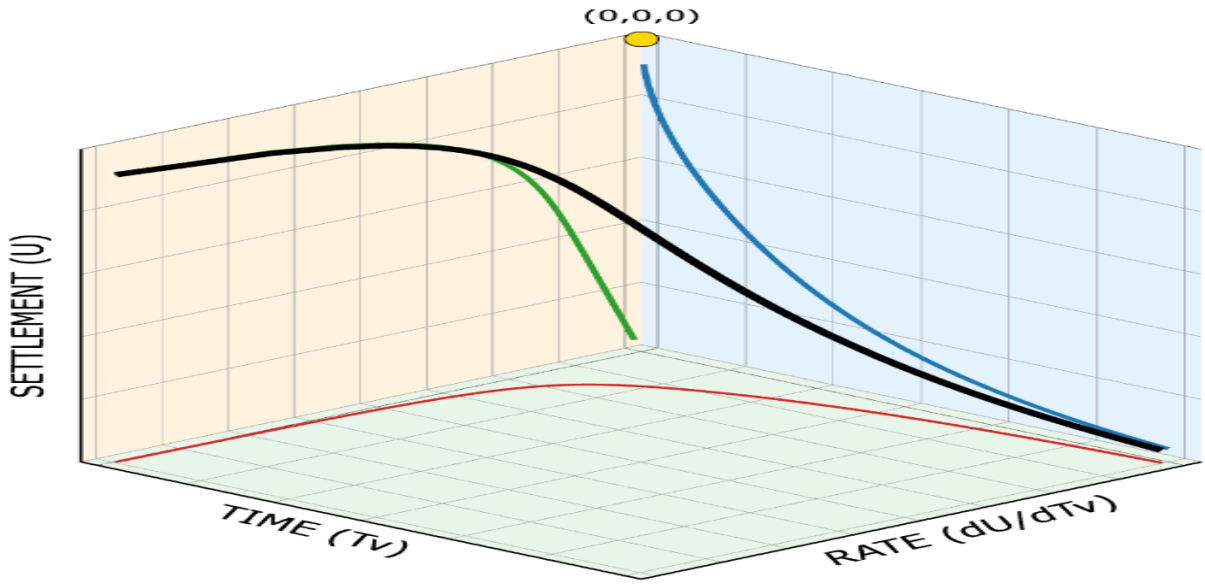

Fig 1. The real 3D Consolidation Path (T-U-U' Black Curve). Blue Wall, Integral Plane (X-Y): Classic Curve (Time vs U; T-U). Orange Wall, Tewatia's Differential Plane (Y-Y'): U vs Rate; U-U'. Green Floor, Newton's Differential Plane (X-Y'): Time vs Rate; T-U'. Origin (0,0,0), U increases downwards 0-1.

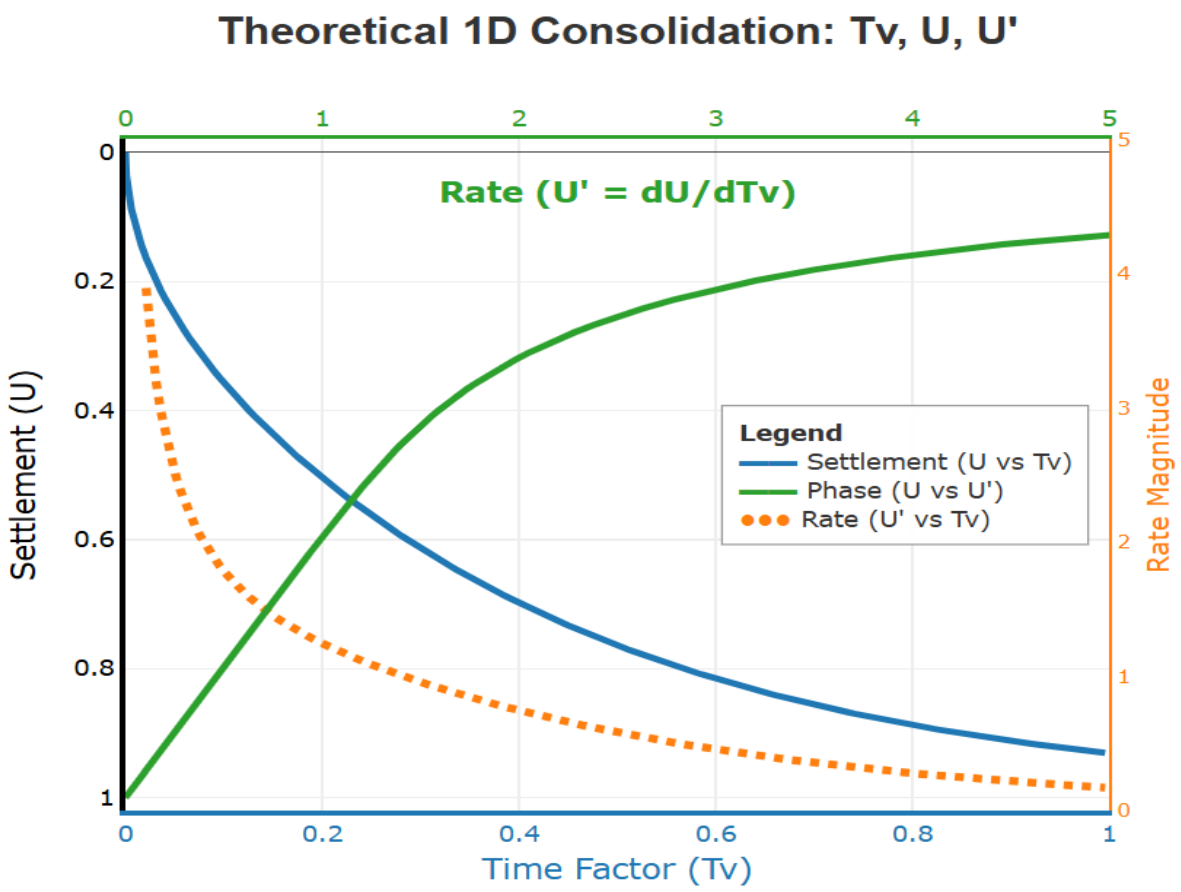

Fig 2. Linear plots of Tv-U (Blue X-Y), Tv-U' (Orange X-Y') & U-U' (Green Y-Y'); where U' = (dU/dTv). They are the projections of real 3D Black Trajectory of Fig 1 on 3 mutually perpendicular (X-Y, X-Y' & Y-Y') planes. Green U-U' curve is a perfect straight line from U = 0.6-1.

phase-space geometry over chronology, the invariant geometric structure—the fundamental DNA—of the soil's hydrodynamic consolidation is mathematically recovered.

This paper introduces the comprehensive theoretical foundations of the Asymptotic Linearity Theorem across three distinct physical phases (Diffusion, Creep, and Compression) and provides the mathematical derivation of the Central Operator, Λ. Furthermore, graph-theoretic principles are applied to stratified media to solve for complex, multi-layered anisotropic conditions. Through rigorous mathematical derivations, step-by-step numerical examples solving the missing time zero problem, and extensive analyses of global real-world infrastructure challenges—including the extreme subcrustal subsidence in Mexico City, coastal sinking in Jakarta, the MOSE floodgate project in Venice, and the historic Leaning Tower of Pisa—this research demonstrates how the X-Y-Y' calculus restores history, predictive modelling, and absolute stability diagnosis to dissipative geotechnical systems where the clock has no zero. Table 1 provides a definitive comparative overview of the fundamental shifts between classical

chronometric modelling and the proposed phase-space geometric modelling.

Table 1. Definite Shifts & Comparison between classical & proposed modelling

Analytical Parameter	Classical Methods	X-Y-Y' Phase-Space Calculus
Primary Independent Variable	Chronological Time (X)	Physical State (Y) and Rate (Y')
Dependent Variable	Settlement Y & Rate Y'	Time, X (derived via geometric integration)
Initial Condition Requirement	Absolute necessity of exact t_0	Completely independent of t_0
Data Visualization Plane	Time vs. Settlement *X vs Y*	Settlement vs. Rate of Settlement *Y vs Y'*
Parameter Extraction Method	Subjective graphical curve-fitting	Direct extraction via snippet of Central Operator slope
Diagnostic Capability	Fails in undocumented historical systems	Reconstructs history and predicts asymptotes

1. Introduction

The rapid, unprecedented expansion of global civil infrastructure, driven by explosive urbanization and compounded by the escalating threats of climate change-induced sea-level rise, has placed severe, unsustainable stress on the geological foundations of the world's megacities. Aggressive, deep groundwater extraction and massive, concentrated structural loading have converged to trigger extreme, catastrophic rates of land subsidence across multiple continents. The underlying geotechnical phenomena driving this subsidence—primarily the hydrodynamic primary consolidation and the secondary visco-plastic creep of highly compressible, fully saturated clay and silt deposits—pose an existential threat to modern civil engineering and urban survival. To mitigate these hazards, prevent structural collapse, and design resilient infrastructure, researchers and engineers have historically relied on mathematical models by Terzaghi (1923), Casagrande (1939), Taylor (1948), Parkin (1978), Olsen (1977), Biot (1941), Carillo (1942), Barron (1948), Leo (2004) etc grounded in classical calculus to predict both the ultimate magnitude and the time-dependent rate of soil settlement [1-9].

However, when these traditional mathematical frameworks are applied to complex, real-world forensic scenarios, they frequently encounter insurmountable conceptual and practical barriers. To fully comprehend why a new mathematical framework is critically necessary for modern geotechnics, one must first confront the foundational limitations of the calculus that has overwhelmingly dominated applied mathematics for over three and a half centuries. Classical calculus, as originally formulated by Isaac Newton and Gottfried Wilhelm Leibniz in the seventeenth century, is fundamentally an analysis of the rates of change over a strictly

chronological continuum. If the variable Y represents a physical state, such as the vertical settlement of a soil layer, and the variable X represents time, Newton's fluxional notation provides the first derivative Y' (the velocity or rate of settlement) and the second derivative Y'' (the acceleration or rate of rate change).

While historically revolutionary and highly successful for certain classes of controlled problems, this framework embeds a profound, restrictive conceptual limitation: it rigidly privileges time as the absolute independent variable and relegates all other physical quantities to a dependent status. When geotechnical engineers plot settlement versus time (the X-Y plane) or the rate of settlement versus time (the X-Y' plane), they are unknowingly observing two-dimensional projections of what is inherently a three-dimensional dynamic phenomenon (Fig 1-2). The true trajectory of any dynamic, dissipative physical system exists in a spatial construct defined by three orthogonal coordinates: the independent variable (typically Time, X), the state variable (Settlement, Y), and the instantaneous rate of change (Velocity, Y'). Classical calculus violently forces the observer to view this three-dimensional reality through flat, two-dimensional shadows, severely obscuring the intrinsic geometric relationship between the state and the rate.

This dimensional incompleteness becomes catastrophic in the field of geotechnical forensics due to the pervasive "Missing Time" problem. Classical consolidation theory is strictly formulated as an initial-value problem. It requires the precise specification of both the governing partial differential equation and the initial boundary conditions at a known, recorded reference time, t_0. While this formulation functions adequately in a highly controlled laboratory oedometer test where a technician can manually start a stopwatch the exact moment a vertical load is applied, the real world does not operate with a clearly defined starting clock. When evaluating a fracturing historical monument, an aging earth-fill highway embankment, or the regional coastal subsidence of an entire geological basin, the precise moment a particular deep clay layer began consolidating is almost always unknown, ambiguous, or physically meaningless. Without a defined t_0, the classical differential equations cannot be solved uniquely, as the constant of integration remains a permanently unknown variable, completely paralyzing the analysis. To resolve this pervasive issue, the geotechnical discipline requires a paradigm shift—a calculus that establishes the internal computational architecture of a dynamic system within its phase-space geometry rather than its chronology (Fig 1-5) [10-12]. This is valid on 3D crack monitoring also that may be seen in sinking or equilibrium achieving infrastructures.

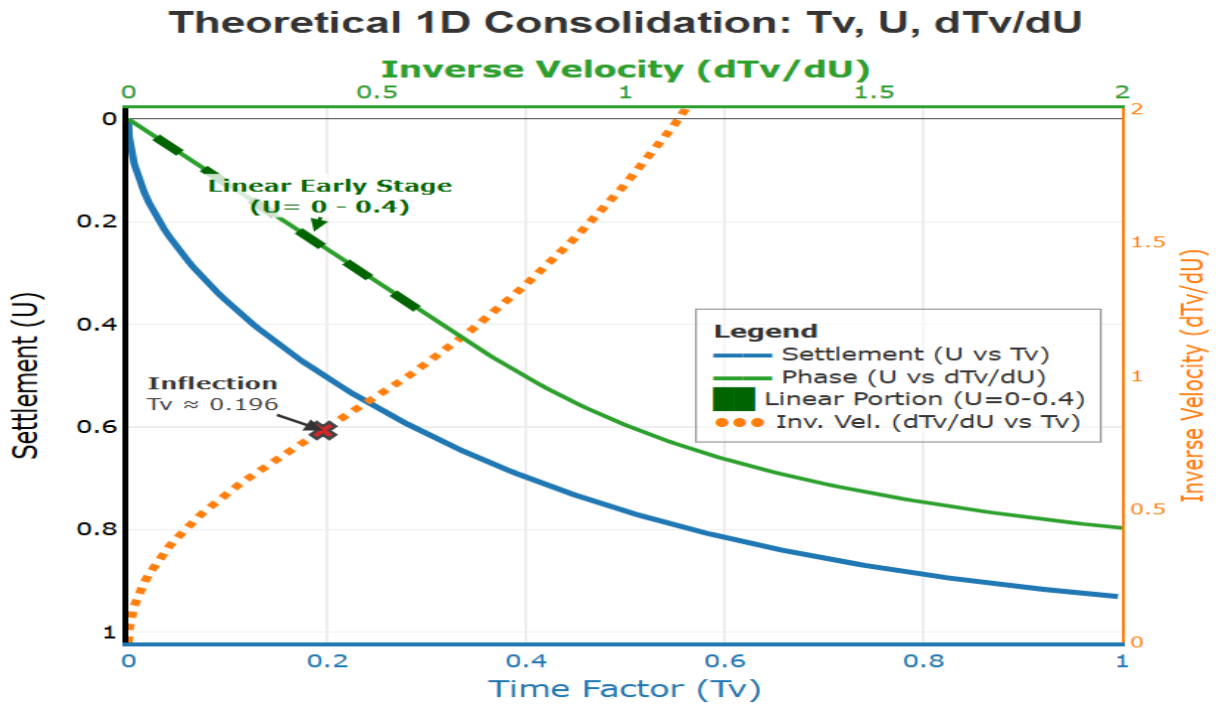

Fig 3. Linear plots of Tv-U (Blue X-Y), Tv-(1/U') (Orange X-Y') & U-(1/U') (Green Y-Y'); where (1/U' = (dTv/dU = Inverse Velocity = U'^{-1} called Inv U'). They are the projections of real 3D Trajectory of Tv-U-U'^{-1} curve in Euclidean space on 3 mutually perpendicular (X-Y, X-Y' & Y-Y') planes. Green U-U'^{-1} curve is a perfect straight line from U = 0-0.4.

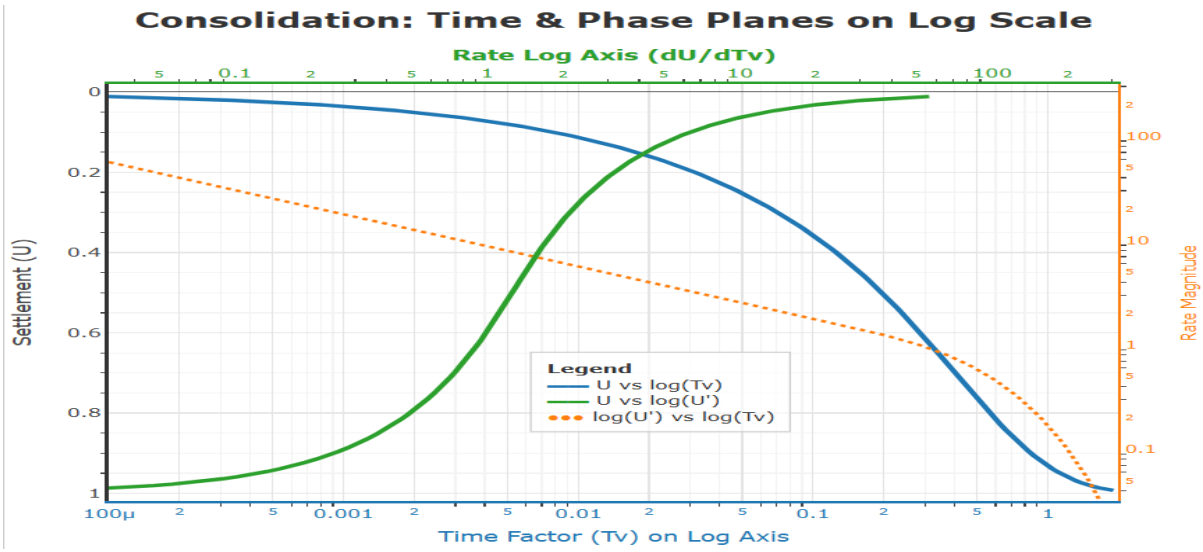

Fig 4. Semi-log plots of U-logTv (Blue Y-logX, the skew S-curve), logU'-logTv (Orange logY'-logX, Parkin 1971 [4]) & U-logU' (Green Y-logY', the symmetrical S-curve, simply called as S-curve henceforth). They are the projections of real 3D Trajectory of U-logTv-logU' curve in Euclidean space on 3 mutually perpendicular (Y-logX, Y-logY' & logY-logY') planes.

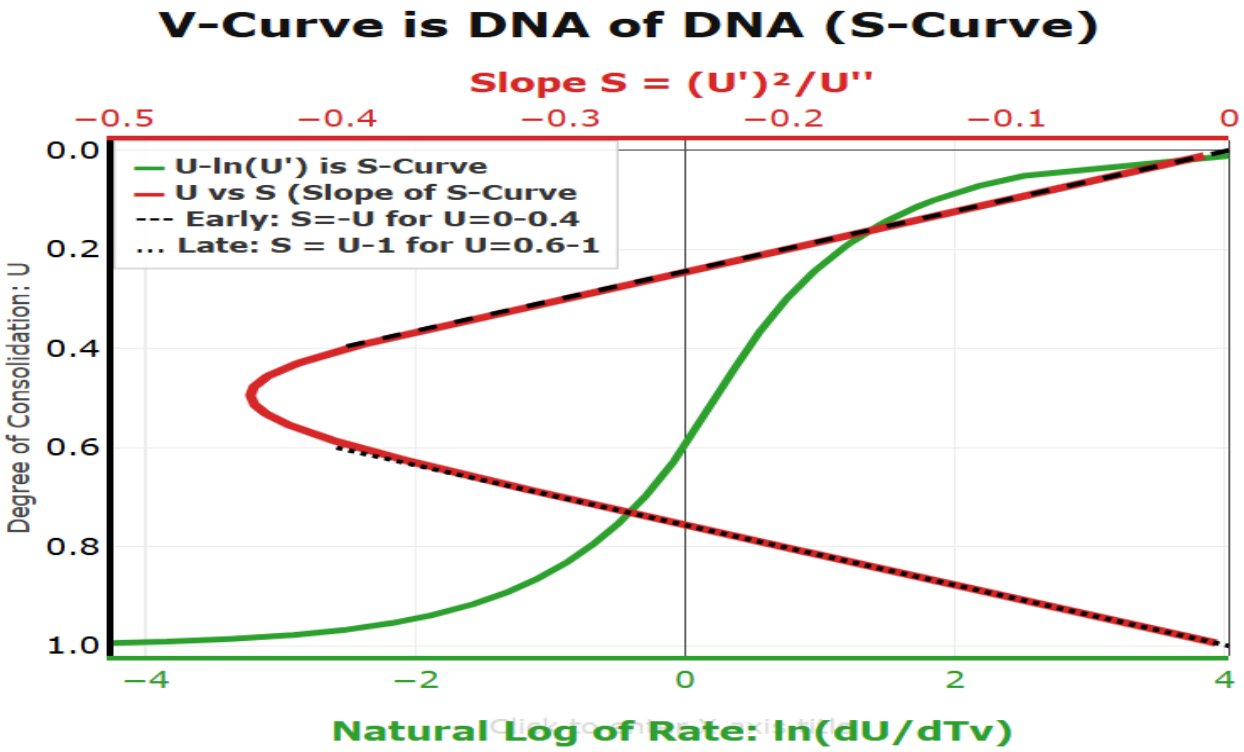

Fig 5. Semi-log plots of U-logU' is the DNA of Eq 3. The Green S- curve has a slope 0.438 on ln and 1 ($=\delta_{100} - \delta_0$) on $\log_{10}$ at U=0.5. The Red curve is linear U-S plot, where S is the slope of S-curve; its DNA of DNA of Eq 3. S = -U for 0<U<0.4 & S = U-1 for 0.6<U<1.

2. History and Evolution of Consolidation Theories

2.1 The Shackles of Classical Mechanics and the 1D Theory

The historical trajectory of dynamic mathematical analysis is deeply rooted in the scientific revolutions of the 1660s and 1670s. Newton's kinematic approach to fluxions was meticulously designed to solve idealized, conservative problems in celestial mechanics, where time was viewed as an absolute, forward-marching, and universally constant variable. For centuries, the primary analytical question asked by scientists and structural engineers was strictly chronometric: predicting precisely where a system would be at a specific future time t_1. It was not until the late nineteenth century, with the advent of Hamiltonian mechanics, statistical thermodynamics, and Henri Poincaré's qualitative theory of dynamic systems, that theoretical mathematicians began to recognize the immense, untapped value of the geometric structure of phase space over pure temporal evolution. Despite these profound advances in theoretical physics and control theory, the time-centric perspective remained deeply and stubbornly entrenched in applied civil and geotechnical engineering, creating a dangerous reliance on

explicit, closed-form solutions that are rarely achievable for complex, heterogeneous natural soils.

The formalization of soil consolidation was achieved in 1923 when Karl von Terzaghi introduced the one-dimensional theory of consolidation [1]. Terzaghi defined soil consolidation as the highly time-dependent process by which the volume of a saturated soil mass decreases due to the gradual expulsion of pore water and the simultaneous dissipation of excess pore water pressure under an applied effective stress. His governing parabolic partial differential equation for one-dimensional vertical consolidation is defined mathematically as:

$$\frac{\partial u}{\partial t} = c_v \frac{\partial^2 u}{\partial z^2} \tag{1}$$

It describes the dissipation of excess pore water pressure u over time t and depth z, where c_v is the coefficient of consolidation, a material property that governs the rate of pore-pressure dissipation. For a soil layer of thickness H with double drainage and an initial uniform excess pore pressure u_0, the Fourier series solution is:

$$u(z,t) = \sum_{m=0}^{\infty} \frac{2u_0}{M} \sin\left(\frac{Mz}{H}\right) \exp(-M^2 T_v) \tag{2}$$

where $M = (2m + 1)\pi/2$ and $T_v = c_v t/H^2$ is the dimensionless time factor. Integrating over the depth to obtain the average degree of consolidation U yields:

$$U = 1 - \sum_{m=0}^{\infty} \frac{2}{M^2} \exp(-M^2 T_v) \tag{3}$$

Terzaghi's brilliant theory is, however, a quintessential example of an initial-value formulation. It demands absolute knowledge of the initial boundary conditions and assumes a perfectly linear relationship between effective stress and the soil void ratio—idealized conditions that rarely exist in natural, highly plastic, and stratified clay deposits. To utilize Terzaghi's theory in practice and extract the vital physical parameter c_v, the global geotechnical industry has relied heavily on two primary graphical curve-fitting techniques: Arthur Casagrande's Logarithm of Time method (1939) [2] and Donald Taylor's Square Root of Time method (1948) [3]. Both established methodologies suffer from severe empirical fragility. They are highly sensitive to subjective curve-fitting errors, user bias, the obscuring phenomenon of initial distortion settlement, and they fail entirely when secondary viscous compression (creep) dominates the primary hydrodynamic phase. Most critically, if the precise start time of the external load application (t_0) is unknown, neither Casagrande's nor Taylor's method can be mathematically initiated.

This infinite series solution Eq 3, while exact, does not immediately reveal the geometric

structure of the consolidation process. However, when we examine the behavior of this solution in different regimes and project it onto the phase plane, distinct geometric signatures emerge (Green curves in Fig 1-5 & Red curve in Fig 5).

2.2 The Genesis of the 3D Triad: Tewatia's 1997-1998 Discoveries [10-11]

The profound paradigm shift required to overcome these historical limitations originated through a series of seminal research papers published in the late 1990s by Prof. Sudhir K. Tewatia, marking the explicit genesis of the 3D triad of Time-Settlement-Slope (X-Y-Y'). In 1997, early research efforts focused intensively on refining classical time-fitting methods, culminating in the publication of the "Improved Root t Method to Evaluate Consolidation Test Results" in the ASTM Geotechnical Testing Journal (GTJ), alongside critical academic discourse regarding the time-dependent behavior of clayey soils. This preliminary work exposed the severe mathematical distortions caused by initial elastic compression and secondary creep when viewed exclusively through the restrictive temporal domain.

The defining historical breakthrough occurred in June 1998 with the landmark ASTM GTJ publication titled "Evaluation of True c_v and Instantaneous c_v, and Isolation of Secondary Consolidation". This foundational paper successfully challenged the century-old reliance on the X-Y and X-Y' temporal planes by explicitly discovering and introducing the missing Y-Y' phase plane to geotechnical engineering. By mathematically isolating secondary consolidation (viscous creep) from primary consolidation utilizing pure rate-based analysis, this publication discovered the "geometric invariant" of dynamic soil systems. The discovery established unequivocally that plotting the State (Settlement, Y) against the Rate (Rate of Settlement, Y') bypassed the need for knowing initial time parameters entirely, proving that the geometry of the deformation curve was an intrinsic physical property independent of the observer's clock. This revolutionary insight was immediately followed by the development of the "T-Chart to evaluate consolidation test results" in September 1998, providing a highly practical graphical tool for engineers to evaluate consolidation without resorting to arbitrary time-fitting abstractions.

2.3 Evolution and Summary of the Rate of Settlement Literature [11-12]

Over the subsequent three decades, the foundational 1998 discovery of the Y-Y' plane evolved into a comprehensive, mathematically rigorous framework, systematically dismantling classical limitations across highly specialized geotechnical and physical challenges. The evolution of this framework is comprehensively documented in the scholarly literature spanning references through [11-12.

Following the introduction of the Y-Y' plane, the methodology was formalized as the "Velocity method for creep and primary consolidation evaluation" (2002), which mathematically bifurcated hydrodynamic pore pressure dissipation from structural visco-plastic behavior. Further

foundational research delineated the "Stress induced time dependent behaviour of clayey soils" (2007) and expanded the rigorous academic discourse on the precise beginning of secondary compression (2006). By 2012, the "Trend of settlement in primary and secondary consolidations" was strictly codified, proving definitively that primary compression yields a linear plot on a standard Cartesian axis, while secondary viscous creep yields a unique linear plot on a semi-logarithmic Y-Y' axis.

The framework was progressively and successfully adapted to highly complex spatial geometries, including the "Equation of 3D consolidation in Cartesian co-ordinates" (2013), which accommodated simultaneous drainage through all six faces of a soil mass. The mathematical isolation of radial consolidation variables was achieved through the introduction of the "U-chart for quick evaluation of radial and 3D consolidation test results" (2013). By analysing the strict geometric equality between the degree of consolidation calculated by vertical settlement and the degree calculated by internal pore pressure dissipation, the framework facilitated the invention of the "Fastest rapid loading methods of vertical and radial consolidations" (2013, 2015). These rapid loading methods revolutionized laboratory and field testing by proving that subsequent load increments could be applied dynamically the moment initial compression was overcome, drastically reducing testing durations from months to days & from days to hours.

The "Principle of super position of rate of settlement in 2D and 3D consolidations" (2015) provided the elegant geometric reasoning required to bypass complex, coupled partial differential equations in multi-directional fluid flow scenarios. Theoretical robustness was continuously validated against emerging complex field conditions, such as the "Consolidation of Clayey Gouge amid Permeating Rock Masses" (2015) and through critical appraisals of the "settlement rate approach" in highly anomalous soils (2019). The complete unification of these decades of rigorous research culminated in the publication of the definitive textbook, *Consolidation of Soils: Rate of Settlement Approach* (2019), and the exhaustive Ph.D. thesis on the *Time Dependent Behaviour of Clayey Soils* (2010). A simple cheapest possible 3D crack monitoring with inbuilt check was suggested in 2006 to replace costly 3D crack monitors to keep an eye on the cracks in infrastructures for safety considerations.

Most recently, the framework was enhanced with advanced computational algorithms, including "Consolidation: Critical Appraisal of Settlement versus Rate of Settlement Approach with Fuzzy Logic" (2022), alongside critical institutional appraisals of vertical consolidation (2022). Ultimately, the mathematical paradigm transcended geotechnical engineering altogether, being formalized as the "Y-Y’ Calculus from Soil Consolidation to other Physical Sciences" (2023), establishing its universal utility in modelling thermodynamics, radioactive decay, cosmology, and any dissipative physical system without ever relying on an initial start time. The historical discussions embedded within this chronological progression solidify the framework's standing as a peer-reviewed, extensively tested paradigm shift in applied mathematics.

3. Theoretical Considerations: The X-Y-Y' Calculus Framework

To overcome the inherent, paralyzing limitations of classical initial-value problems, the X-Y-Y' framework completely reverses the traditional analytical flow, constructing a rigorous, mathematically sound geometry of change.

3.1 Dismantling the Cartesian Plane: Vector Representation in 3D Space

The calculus begins by completely dismantling the conventional two-dimensional Cartesian plane and erecting a formal three-dimensional Euclidean structure to define the System Space. This space is characterized by three mutually orthogonal axes:

Axis X (The Independent Variable): Represents the progression parameter. While classically restricted to Time (t), it can represent any independent coordinate such as spatial progression or load increments. Notation: $X \in R$

Axis Y (The Dependent State): Represents the observable, measurable physical quantity of the system, such as vertical settlement (δ), temperature, or concentration. Notation: $Y = f(X)$.

Axis Y' (The Rate of Change): Represents the instantaneous rate of change of the state variable with respect to the progression parameter, such as the velocity of settlement ($v = d\delta/dt$) or heat flux. Notation: $Y' = dY/dX$.

The complete mechanical state of the dynamic consolidation process at any specific instant is not a simple coordinate pair, but a continuous, dynamic position vector $r(X)$ tracing a definitive curve in three-dimensional space:

$$\overrightarrow{\boldsymbol{r}(\boldsymbol{X})} = \boldsymbol{X}\hat{\boldsymbol{\imath}} + \boldsymbol{f}(\boldsymbol{X})\hat{\boldsymbol{\jmath}} + \boldsymbol{f}'(\boldsymbol{X})\hat{\boldsymbol{k}} = \boldsymbol{X}\hat{\boldsymbol{\imath}} + \boldsymbol{Y}(\boldsymbol{X})\hat{\boldsymbol{\jmath}} + \boldsymbol{Y}'(\boldsymbol{X})\hat{\boldsymbol{k}} \tag{4}$$

where $\hat{\boldsymbol{\imath}}, \hat{\boldsymbol{\jmath}}$ **and** $\hat{\boldsymbol{k}}$ are the standard unit vectors. Any two-dimensional projection of this specific curve (such as the standard time-settlement plot) represents a partial, fundamentally incomplete view that necessarily discards critical mechanical information regarding the system's velocity architecture.

3.2 The Fundamental Inversion: Prioritizing State and Rate

The central, revolutionary thesis of the Y-Y' framework is that time is a mathematical consequence of physical motion, not the physical cause of it. In dissipative systems, the soil matrix evolves because it is seeking a state of mechanical equilibrium with an external effective stress, not because a clock is advancing on the wall. In the classical Newtonian framework, the analytical sequence is rigid and fragile: Define Time (X), Observe State (Y), Derive Rate (Y').

The X-Y-Y' framework executes a fundamental inversion. The new analytical sequence dictates: Define the independent observable variables (State, Y, and Rate, Y'); Plot the Phase Plane

Trajectory mapping *Y* against *Y'*; and mathematically derive Time (*X*) as a dependent consequence of the resulting geometric shape. By substituting the Rate (*Y'*) in place of Time (*X*) as the primary axis of analysis, the trajectory in the Tewatia's *Y-Y'* plane (the Phase Plane) becomes a solid, time-invariant geometric signature. Because this geometric relationship between the state and the rate is an intrinsic physical property of fluid diffusion and skeletal compression, it remains an absolute, unalterable truth regardless of when the observer started recording data.

3.3 Transformation of Differential Equations

The integration of classical derivatives into phase-space geometry relies on the chain rule to bridge acceleration, velocity, and geometric slope. By definition, the rate of change of the rate is acceleration: $\boldsymbol{Y'' = d^2Y/dX^2 = dY'/dX}$. Furthermore, the geometric slope of the Y-Y' trajectory is defined mathematically as $\boldsymbol{dY'/dY}$. Applying the chain rule:

$$\frac{dY'}{dY} = \frac{dY'/dX}{dY/dX} = \frac{Y''}{Y'} \qquad or \quad Y'' = Y'.\frac{dY'}{dY} \tag{5}$$

This fundamental transformation relationship proves mathematically that the second derivative (the acceleration of settlement) is strictly equal to the first derivative (the velocity of settlement) multiplied by the geometric slope of the Y-Y' phase trajectory. Consequently, any complex second-order autonomous differential equation of the form $\boldsymbol{d^2Y/dX^2 = G(Y, Y')}$ can be elegantly and simply transformed into a first-order equation in the Y-Y' plane: $\boldsymbol{Y'.(dY'/dY) = G(Y, Y')}$.

Tewatia (2012) [11-12] used this property to derive Barron's (1948) Equation of Radial Consolidation & Carillo's Equation of combined Vertical + Radial Consolidation in simple and short manner with school level math without using partial differential equations. The 3D consolidation Eq in Cartesian Coordinates did not exist in literature, where a parallelopiped sample drains from all six phases with different permeabilities in X, Y, Z directions. This too was derived easily by Tewatia (2013) by school math [11]. Not only 3D, but analogy was also extended to N-dimensions in electricity in RC circuits [12].

4. The Asymptotic Linearity Theorem (ALT): The Quinity of Deformation

A foundational pillar of the Y-Y' calculus, which enables its immense predictive power across disciplines, is the Asymptotic Linearity Theorem (ALT). When an external load is applied to a highly heterogeneous soil mass, the initial transient consolidation behavior is highly complex, involving multiple interacting drainage paths, elastic structural distortion, and anisotropic fluid flow. Classical time plots display this as a mathematically cumbersome curve. However, the ALT establishes that for any diffusion process occurring within a bounded domain governed by

parabolic partial differential equations, the trajectory in the phase plane asymptotically approaches a universal straight line, completely regardless of the initial boundary complexity or spatial heterogeneity.

The system reveals five distinct, mathematically rigorous types of asymptotic linearity, forming a complete quinity that exposes the geometric DNA of the consolidation process; 3 in Diffusion, 4th in Creep and 5th in Compression (Index).

4.1 Type I: Diffusion on Linear δ-(dδ/dt) Scale (Late Phase U>0.6)

For large values of T_v (typically $U > 0.6$), the higher-order terms in the Fourier series (Equation 4.3) decay exponentially and become negligible. Retaining only the first term ($m = 0$, $M = \pi/2$):

$$U = 1 - \frac{8}{\pi^2}\exp\left(-\frac{\pi^2}{4}T_v\right) \tag{6}$$

Taking the derivative with respect to T_v & Rearranging:

$$\frac{dU}{dT_v} = -\frac{\pi^2}{4}U + \frac{\pi^2}{4} \tag{7}$$

This is a linear relationship between U and dU/dT_v in the phase plane. This result constitutes the Asymptotic Linearity Theorem: in the late stages of primary consolidation, the trajectory in the Y-Y′ phase plane approaches a straight line with slope $-\pi^2/4 \approx -2.467$. This geometric signature is profound. It means that regardless of the initial conditions, boundary conditions, or drainage configuration (provided the system obeys the one-dimensional diffusion equation), the late-stage trajectory will asymptotically approach a universal straight line in the phase plane. The slope of this line (Fig 2 Green Curve) is the Central Operator $\Lambda = \pi^2/4$, a fundamental constant that encodes the diffusion physics. The intercept of *δ-(dδ/dt)* line on *δ-axis* where velocity or rate of settlement $d\delta/dt = 0$, gives the ultimate settlement, δ_{100} (Fig 6)

$$\frac{d\delta}{dt} = -\Lambda\frac{c_v}{H^2}(\delta - \delta_{100}) \quad or \quad \delta = -\frac{H^2}{\Lambda c_v}\frac{d\delta}{dt} + \delta_{100} \tag{8}$$

4.2 Type II: Diffusion on Linear *δ*-(dt/*dδ*) Scale (Early Phase U<0.4)

In the early parabolic phase of consolidation, governed strictly by Terzaghi's hydrodynamic diffusion equation, the relationship between settlement (δ) and the inverse velocity ($dt/d\delta$) is strictly linear on regular Cartesian coordinates. This represents pure hydrodynamic pore water expulsion. The infinite series solution for small degrees of consolidation ($U<0.4$) simplifies to a parabolic law: $Tv = (\pi/4)U^2$. Differentiating & re-arranging yields the fundamental linear relationship:

$$\delta = k\,\frac{dt}{d\delta} + \delta_0 \tag{9}$$

where the constant slope is defined as

$$k = \frac{8}{\pi}\,\frac{(\delta_{100}-\delta_0)^2 c_v}{H^2} \tag{10}$$

This Type II linearity emerges within minutes of initial loading, allowing for the immediate extraction of the coefficient of consolidation (c_v) and the unknown initial settlement (δ_0), serving as a powerful real-time quality control diagnostic. Where, (δ_{100} - δ_0) = s_{50}, the slope of *Semi-Log δ-(dδ/dt) Plot at U = 0.5 = 50%.* This comes from Eq 11-12.

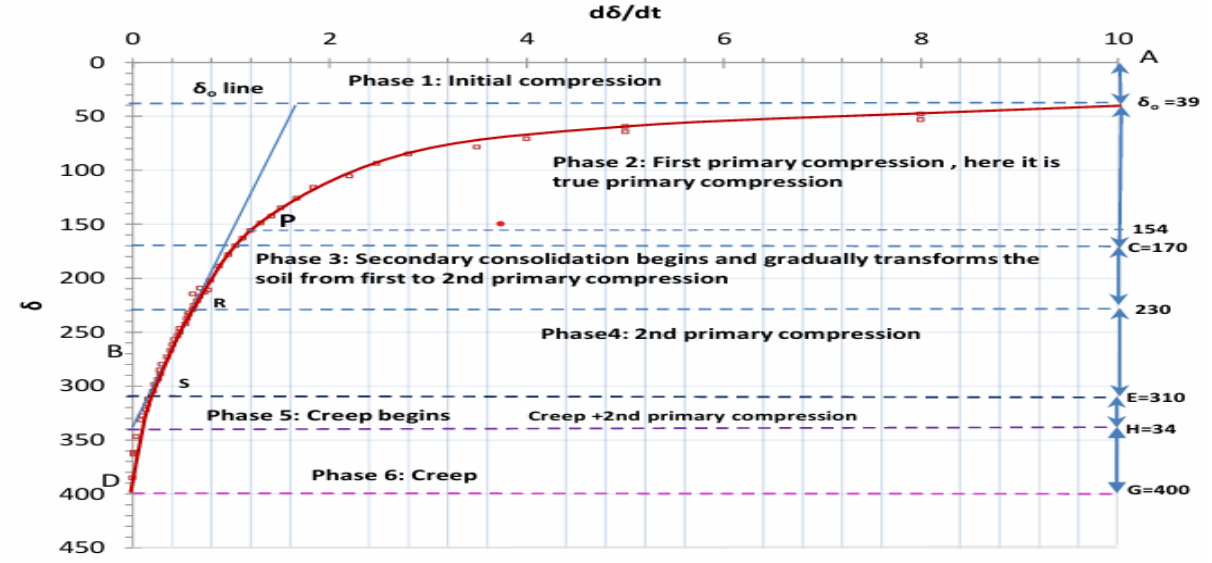

Fig 6. Data filtration & Evaluation by the δ- dδ/dt plot of Sawan Bhadon Dam Soil. The blue straight-line slope provides *Cv* and its intercept on δ-axis is δ_{100}.

4.3 Type III: Diffusion on Semi-Log Scale (S-curve & Mid Phase 0.4 < U < 0.6)

While the early-stage and the late-stage linear signature provide powerful tools for analysing the extremes of the consolidation process, a complete picture requires a representation that captures the entire trajectory from $U = 0$ to $U = 1$. This is achieved by plotting U versus $\ln(dU/dT_v)$ in a semi-logarithmic phase plane, Fig 4-5. In this representation, the consolidation trajectory exhibits a remarkable symmetry. The curve transitions from convex ($0 < U < 0.5$) to concave ($0.5 < U < 1$), with the inflection point occurring precisely at $U = 0.5$. This symmetry is a direct consequence of the mathematical structure of the Fourier series solution (Fig 7).

4.3.1 Theoretical Values at 50% Consolidation

At $U = 0.5$, the theoretical values derived from Eq 3 are: $T_{50} = 0.197$, $\left(\frac{dU}{dT_v}\right)_{50} = 1.256$

The slope of the U versus $\ln(dU/dT_v)$ curve at $U = 0.5$ can be shown to be:

$$S_{50} = \frac{dU}{d[\ln(dU/dT_v)]}_{U=0.5} \approx -0.438(\text{natural log}) \tag{11}$$

$$S_{50} \approx -1.009 \approx -1.0(\text{base-10 log}) \tag{12}$$

This universal slope of approximately −1.0 on a base-10 semi-logarithmic plot provides a quick visual check of whether experimental data conform to the theoretical S-curve. Significant deviations from this slope at 50% consolidation indicate departures from ideal Terzaghian behavior, such as the presence of secondary compression, non-uniform initial pore-pressure distributions, or boundary effects.

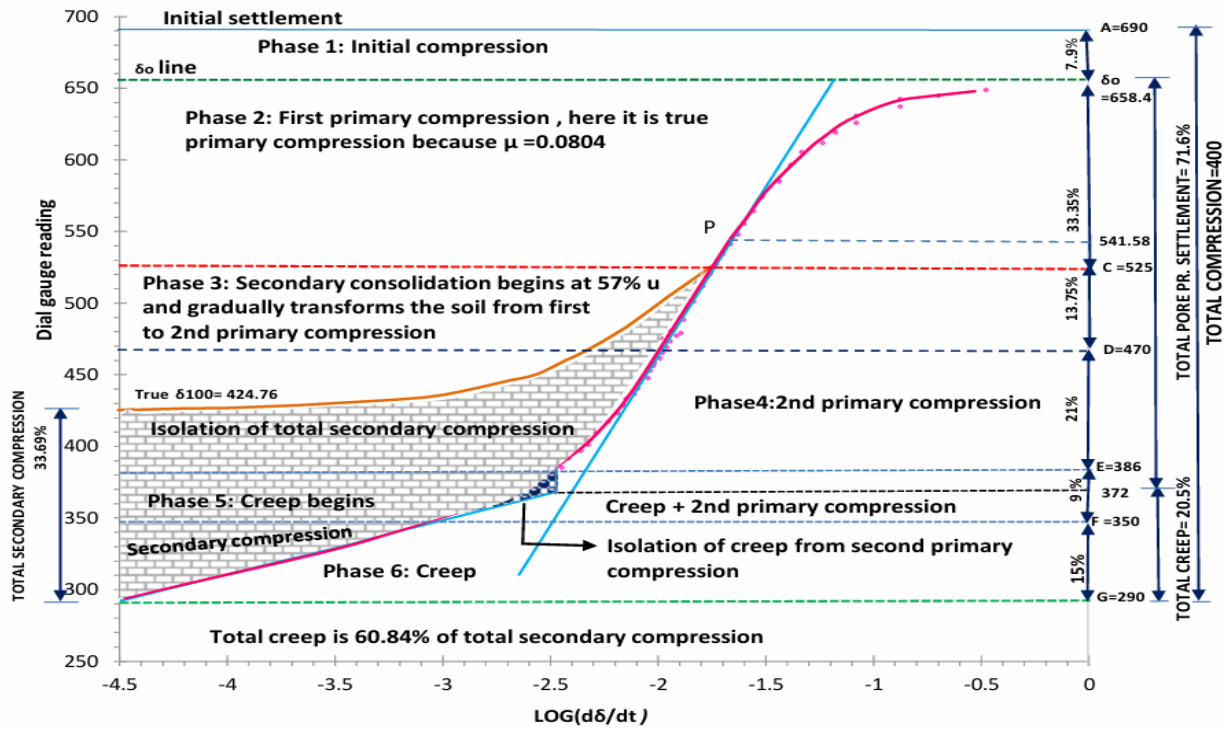

Fig. 7. Evaluation & Filtration: The δ-log(dδ/dt) plot for Sawan Bhadon soil shows complete isolation of Initial, 1st Primary, 1st Transition, 2nd Primary, 2nd Transition, The consolidation parameters along with the in-built check on data, μ, can be easily evaluated as per the suggested method.

4.3.2 The Pivot Point and Symmetry

The 50% consolidation point serves as a pivot in the phase-plane trajectory. The convex-to-concave transition at this point reflects the underlying symmetry of the diffusion equation: the process of approaching equilibrium from below ($U < 0.5$) mirrors the process of approaching equilibrium from above ($U > 0.5$), with time running in opposite directions. This symmetry has deep connections to the mathematical properties of the diffusion operator. The Fourier series

solution (Eq 3) can be rewritten in terms of the complementary degree of consolidation $\bar{U} = 1 - U$:

$$\bar{U} = \sum_{m=0}^{\infty} \frac{2}{M^2} \exp(-M^2 T_v) \tag{13}$$

The symmetry between U and $\bar{U}$ manifests geometrically in the phase plane as the mirror symmetry of the S-curve about the 50% point.

4.3.3 The Truth Check (μ) - A Quality Control Metric: Derivation

The geometric signatures described above—the V-curve (Fig 5), the linear signature, and the S-curve—are all manifestations of the same underlying diffusion physics. If a soil truly obeys Terzaghi's one-dimensional diffusion equation (i.e., exhibits pure Terzaghian behavior), then these signatures must be mutually consistent. The Truth Check (μ) is a dimensionless parameter that quantifies this consistency. The derivation begins with two independent expressions for the coefficient of consolidation c_v, both evaluated at $U = 0.5$. From the standard time-factor relationship (Casagrande 1939) [2]:

$$c_v = \frac{0.197 \cdot H^2}{t_{50}} \tag{14}$$

From the phase-plane analysis, using the slope S_{50} and rate $(dU/dT_v)_{50}$ at 50% consolidation: The ratio $|S_{50}|/(dU/dT_v)_{50}$ can be shown to equal 0.8033 from the theoretical values in Eq 11-12. This leads to:

$$c_v = \frac{0.8033 \cdot (dU/dT_v)_{50} \cdot H^2}{|S_{50}|} \tag{15}$$

Converting to dimensional form with $v_{50} = (d\delta/dt)_{50}$ and $s_{50} = |S_{50}|$ (the magnitude of the slope in dimensional units):

$$c_v = \frac{0.8033 \cdot v_{50} \cdot H^2}{s_{50}} \tag{16}$$

Equating Eq 14 & 16

$$\frac{0.197 \cdot H^2}{t_{50}} = \frac{0.8033 \cdot v_{50} \cdot H^2}{s_{50}}$$

Simplifying:

$$\frac{t_{50} \cdot v_{50}}{s_{50}} = \frac{0.197}{0.8033} \approx 0.245$$

However, the conventional formulation normalizes this to a dimensionless ratio by dividing by a constant factor. The Truth Check is defined as [10-12]:

$$\mu = \frac{t_{50} \cdot v_{50}}{0.245 \cdot s_{50}} \tag{17}$$

where the constant 0.245 is chosen such that μ = 1.0 for ideal Terzaghian behavior.

4.4 Type IV: Creep on Semi-Log Scale (Late Phase, near or after the end of Primary Consolidation)

After primary consolidation is substantially complete (typically *U>0.9* for inorganic soils) and excess pore pressure has fully dissipated ($u_e \approx 0$), the soil skeleton undergoes purely viscous deformation under sustained effective stress. The empirical creep law follows: $\delta = a.ln(t) + b$. Differentiating and expressing it within the phase plane reveals a strictly linear relationship on semi-logarithmic coordinates:

$$\delta = a.\ln\left(\frac{dt}{d\delta}\right) + b + a.lna \tag{18}$$

This geometric relationship produces a straight line perfectly parallel to the classical δ-ln(t) compression curve, separated by a distinct horizontal distance of *ln(a)* or vertical distance a.ln(a); Fig 8.

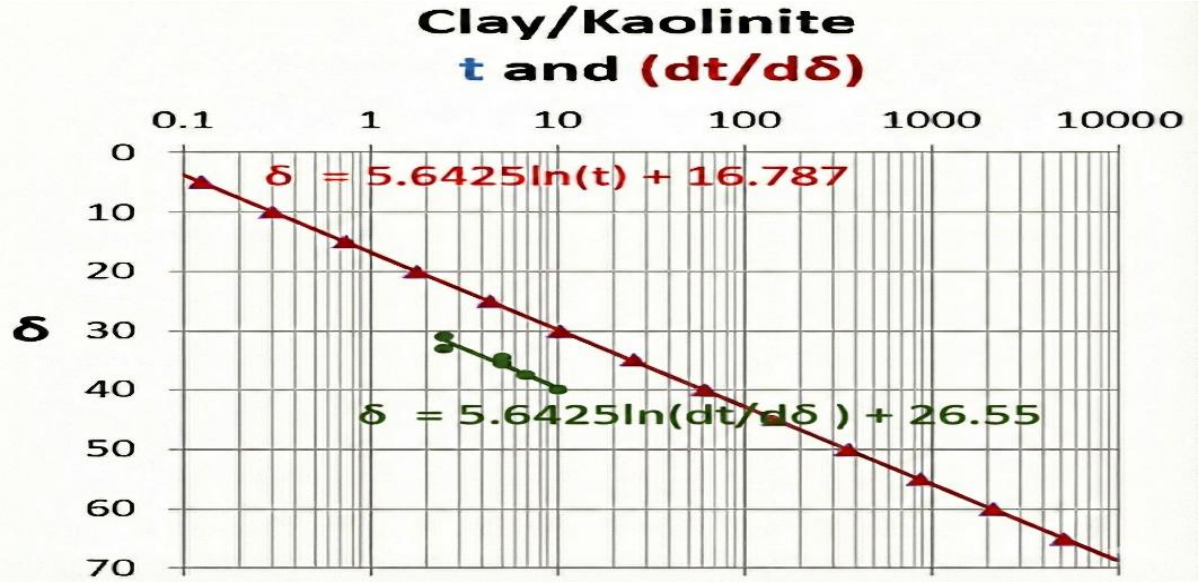

Fig 8. Retrieving the past, present & future *δ-t* data (of old structures like Pisa tower) from the snippet of *δ-(dt/dδ)* plot by simple graphical integration and extracting *α* when initial and boundary conditions are unknown. Unlike, classical calculus, no constant of integration is required in Tewatia's Y-Y' calculus.

$$\alpha = -\ln(10) \cdot LC \frac{1+ef}{h_f} \times (a) \tag{19}$$

Where, a is the slope of δ-$ln(t)$ or δ-$log(dt/d\delta$ plots, α is the coefficient of secondary consolidation (slope of e-$log_{10}(t)$ plot); h_f & e_f are final height &final voids ratio of the soil, LC is the least count of settlement measuring instrument (Tewatia et al 2007). The slope ***a*** contains the geometric fingerprint, inherent "viscosity DNA" of the soil structure.

4.5 Type V: Compression on Semi-Log Scale (Pressure, Loading Phase)

Mostly, in the active loading phase, the relationship between settlement and the logarithm of the effective pressure rate ($\delta = A.ln(\sigma') + B$) is brilliantly linear on semi-log coordinates. This captures the exponential stiffening behavior of the soil matrix as it compresses under load.

Differentiating the classical compression curve with respect to pressure & re-arranging reveals the geometric truth:

$$\delta = A.\ln\left(\frac{d\sigma\prime}{d\delta}\right) + B + A.lnA \tag{20}$$

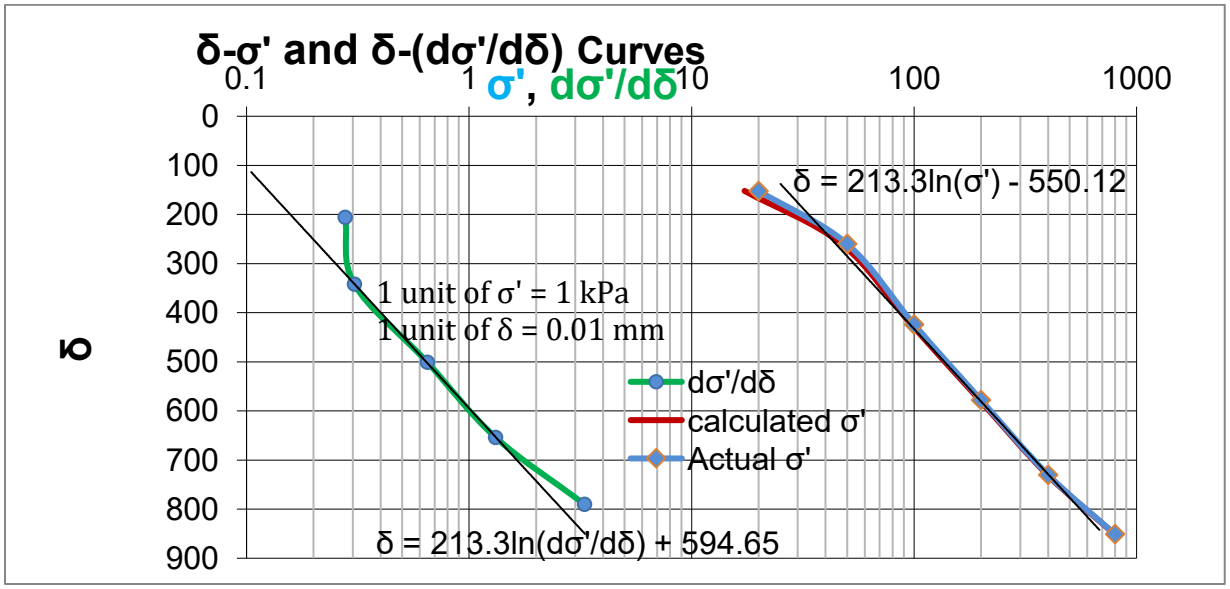

Fig 9: Comparison of generated δ-σ' data with actual δ-σ' data

This geometric relationship produces a straight line perfectly parallel to the classical compression curve, separated by a distinct horizontal distance of $ln(A)$. The slope enables the direct determination of the compression index (Cc) and the mathematical back-calculation of the completely unknown initial effective pressure (σ'_0) without ever requiring the complete loading history. Fig 9 shows the validity & proof of this method where generated data completely matches with the actual data (Tewatia el 2014).

5 Radial Consolidation, Linearity Onset and Combined Drainage

A critical, revolutionary discovery within the framework corrects a widespread classical misconception: radial consolidation does not wait until 50% or 60% completion to become mathematically linear. Instead, radial drainage exhibits asymptotic linearity from the very beginning—as early as 5-10% consolidation. This occurs because the mathematical solution for radial consolidation consists of a single exponential decay function without the complex, higher-order Fourier series terms found in vertical consolidation models, Fig 10.

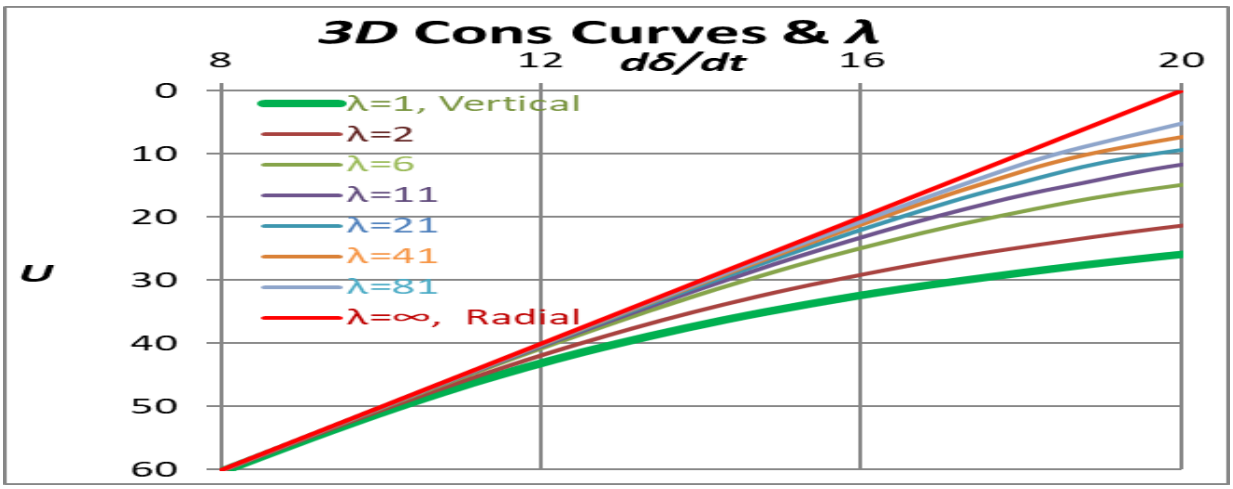

Fig 10. Asymptotic Linearity Theorem: Radial consolidation on Tewatia's Y-Y' plane is a straight line right since beginning, while Vertical consolidation becomes linear at 60% U. In combined vertical and radial (3D) consolidation, λ (varies 1-∞) determines the dominance of radial consolidation over vertical consolidation. But whatever is λ, any combination of consolidation becomes linear latest by 60% U or earlier.

For combined vertical-radial consolidation—the most prevalent scenario in global infrastructure projects utilizing prefabricated vertical drains (PVDs)—Carillo's equation $\{1-U_{rv} = (1-U_r)(1-U_v)\}$ dictates the overall degree of consolidation. In the Y-Y' phase plane, this is derived purely geometrically through the harmonic addition of time scales, where discharge rates are strictly non-interfering and additive $(d\delta/dt)_{rv} = (d\delta/dt)_r + (d\delta/dt)_v$. The onset of asymptotic linearity in combined systems is strictly dependent on the anisotropy ratio

$$\lambda = 1 + \frac{32k_rH^2}{\pi^2 k_v {d_e}^2 F_n} \tag{21}$$

For typical, well-designed drain systems where λ ranges from 10 to 20, linearity emerges rapidly at just 20-30% consolidation. In intensive drainage scenarios (where λ>100), linearity emerges at a mere 10-15% consolidation. This allows critical design parameters to be verified in the field within days rather than months, accelerating construction schedules up to ten times faster than

classical models permit.

6. The Central Operator (Λ)

If the Y-Y' phase plane provides the precise map of the soil's behavior, the Central Operator, Λ serves as the absolute compass. For any linear dissipative system, the complex differential governing equation reduces in the phase plane to a strictly linear algebraic form: $Y' = -\Lambda. Y + C.$ The Central Operator is a composite scalar value representing the exact slope of the linear trajectory in the Y-Y' plane, containing all the intrinsic physical constants of the specific system. For one-dimensional vertical consolidation, the Central Operator (Type I) is directly proportional to the coefficient of consolidation and inversely proportional to the square of the drainage path length:

$$\Lambda = \frac{\pi^2 C_v}{4H^2} \tag{22}$$

By plotting the observed current settlement, Y against the measured current rate of settlement, Y' and calculating the slope of the resulting straight line, the geotechnical engineer extracts the soil's true hydrodynamic properties directly from the raw data. The Central Operator for Type IV (Creep) is simply a, representing the viscosity DNA, while for Type V (Compression), it is A, representing the compressibility DNA. This fundamentally eliminates the need for arbitrary "time factors" (like T_{50}, t_{50} or T_{90}, t_{90}) and subjective visual curve-matching like in Casagrande & Taylor Methods [2,3]. Continuous linearity of data points in the specified domain (say, $U>0.6$) automatically provides quality check on observations and soil's theoretical behavior & only a data snippet is enough to evaluate consolidation parameters.

7. Graph Theory in Stratified Media under Complex Anisotropic Conditions

Real geological soil profiles are highly stratified and complex, rarely conforming to the homogeneous assumptions required by classical calculus. Classical analysis attempts to treat this as an intractable boundary value problem with complex interface conditions between varying soil types. The X-Y-Y' framework introduces an elegant graph-theoretic formulation to resolve this complexity mathematically. In this specific network representation, each distinct soil layer is modelled as a discrete "node" characterized by its exact thickness (h_i), consolidation coefficient ($C_{v,i}$), and permeability (k_i). The physical hydraulic connections between adjacent layers act as "edges" with specific conductance weights ($w_{i,j}$) representing the true hydraulic coupling. The system's ultimate asymptotic behavior is defined by the Dominant Node Theorem, which mathematically proves that in any multi-layer system, there exists a single, critical layer that completely controls the long-term consolidation trajectory of the entire strata.

The dominant node is identified mathematically as the layer possessing the maximum absolute

hydraulic resistance ($R_i = h_i^2/C_{v,i}$). The full consolidation dynamics satisfy the matrix eigenvalue problem $du/dt = -Gu$, where G is the system's conductance matrix. The absolute smallest eigenvalue (λ_1) represents the slowest decay mode, dictated entirely by the dominant node. Consequently, as time $t \to \infty$, the entire stratified system behaves asymptotically as a simple single-layer system controlled entirely by the properties of the most restrictive, dominant layer. In the Y-Y' phase plane, the geometric slope of the linear trajectory perfectly aligns with λ_1, providing a rigorous, simple method to analyze complex anisotropic environments.

8. Numerical Examples: Solving the Missing Time Zero Problem

The most significant practical triumph of the X-Y-Y' calculus is its proven ability to mathematically reconstruct the chronological timeline of a deformation event without ever having witnessed its beginning, thereby permanently solving the Missing Time problem.

In classical Newtonian calculus, velocity is defined strictly forward in time as $v = dy/dt$, requiring the forward integration $y(t) = \int v(t)dt + C$. If the initial starting time (tied directly to the integration constant C) is unknown, the equation is permanently, mathematically unsolvable. The X-Y-Y' calculus sidesteps this barrier by rearranging the fundamental mathematical definition to make Time the isolated subject: $dt = dy/v$. By integrating the inverse of the velocity with respect to the evolving physical state, the exact elapsed time can be precisely recovered:

$$t = \int \frac{1}{v(y)} dy \tag{23}$$

Geometrically, this implies that calculating the area under the curve in a secondary plot of State (Y) versus the Inverse Rate ($1/Y'$) directly yields the elapsed Time (X).

8.1 Example 1: The Unknown Highway Embankment

Consider a complex forensic assessment of a highway embankment constructed over a deep layer of normally consolidated clay. The embankment was built several years prior, but original construction records, loading conditions, and exact start dates (t_0) were destroyed or unrecorded. A modern structural monitoring program measures current settlement (δ) to determine the velocity of settlement ($v = d\delta/dt$).

Field Data Extraction:

- At monitoring instance 1, the accumulated settlement is recorded as $\delta_1 = 1.20$ meters, and the downward velocity is $v_1 = 0.05$ meters/month.
- At monitoring instance 2, the settlement reaches $\delta_2 = 1.35$ meters, and the velocity has predictably slowed to $v_2 = 0.02$ meters/month.

Step 1: Identifying the Central Operator (Λ)

The investigating engineer bypasses the time domain entirely and plots State against Rate. Utilizing the Asymptotic Linearity Theorem (since velocity is decreasing linearly with settlement), the Central Operator is calculated exactly as the geometric slope:

$$\Lambda = \left|\frac{v_2 - v_1}{\delta_2 - \delta_1}\right| = \left|\frac{0.02 - 0.05}{1.35 - 1.20}\right| = \left|\frac{-0.03}{0.15}\right| = 0.20\ months^{-1}$$

Step 2: Predicting Ultimate Primary Settlement (δ_{100})

The ultimate primary settlement limit is reached when the velocity reaches an absolute zero ($v=0$). Utilizing the point-slope linear equation derived from the phase plane:

$v_2 - 0 = -\Lambda(\delta_2 - \delta_{100})$ ➔ $0.02 = -0.20(1.35 - \delta_{100})$ ➔ $\delta_{100} = 1.35 + 0.10 = 1.45$ meters

Without knowing the initial load or any historical data, the embankment is proven mathematically to settle exactly an additional 10 cm before primary consolidation completely ceases.

Step 3: Recovering the Missing Time ($t_{elapsed}$) To determine the historical timeline and confirm the age of the structure, the engineer integrates the inverse rate from the hypothetical zero-settlement state to the current state:

$$t = \int_0^{1.35} \frac{1}{\Lambda(\delta_{100} - \delta)}\, d\delta = \frac{1}{0.20}\, ln\left(\frac{1.45}{1.45 - 1.35}\right)$$

$$t = 5 \cdot ln(14.5) = 5 \cdot 2.674 = 13.37 \text{ months}$$

The load was applied exactly 13.37 months prior to the second instrument reading. The engineer has mathematically reconstructed history without a clock.

8.2 Example 2: Complex Anisotropic Stratified Profile

A critical offshore structure rests on a highly variable three-layer stratified soil profile composed of sand, soft marine clay, and dense silt, fitted extensively with radial PVD drains to accelerate consolidation. Classical partial differential equations fail due to highly anisotropic flow and completely unknown interface conductivities.

Applying the X-Y-Y' framework, the engineer treats the stratified media strictly as a hydraulic graph. The marine clay layer is identified mathematically as the Dominant Node, possessing the highest hydraulic resistance $\boldsymbol{R_{clay} = \max(h_i^2/C_{v,i})}$. Because radial consolidation linearity is achieved at just 15% consolidation, and the combined anisotropy parameter, λ from Eq 21 is determined to be 15, the overall system achieves asymptotic linearity at 30% consolidation.[1] By

plotting the early settlement rate readings from field extensometers into the Y-Y' plane, the combined Central Operator is extracted directly from the geometric slope, enabling precise 50-year structural settlement forecasting within just three weeks of initial loading, entirely bypassing the need for complex numerical finite element modelling.

9. Global Scope to Infrastructure Challenges

The theoretical supremacy of the X-Y-Y' calculus is unequivocally validated by its application to the world's most severe, highly publicized, and well-documented geotechnical crises. In these vulnerable megacities, traditional initial-value calculus has repeatedly failed due to unprecedented physical scale, profound historical ambiguity, and complex non-linear visco-plastic soil behaviors.

9.1 Mexico City: The Subcrustal Collapse

Mexico City represents arguably the most extreme and catastrophic case of human-induced land subsidence on the planet. Built directly upon the drained, highly saturated bed of the ancient Lake Texcoco, the city's subsoil consists of extraordinary volcanic clays with initial void ratios frequently exceeding an astonishing 5.0. Driven by aggressive deep groundwater extraction required to support a metropolitan population of over 20 million, the historical settlement rates are staggering, surpassing 8 meters cumulatively over the last century. The Palacio de Bellas Artes, a massive marble cultural centre in the heart of the city, provides a quintessential example of the Missing Time problem. Construction began in 1904, was interrupted for decades by the Mexican Revolution, and was completed in 1934. The building has sunk more than 4.6 meters, completely submerging its original ground floor.[1] Because t_0 and the initial boundary stresses are entirely ambiguous due to sporadic, asymmetric loading over 30 years, classical explicit solutions fail. By deploying the X-Y-Y' calculus and plotting the current settlement of the Palacio against its current velocity of settlement (captured via modern LiDAR arrays), engineers identify the Central Operator directly from the phase plane trajectory. The ALT allows for highly accurate projections of ultimate future settlements based solely on the current geometric deformation signature, providing crucial intelligence for architectural conservation efforts without needing to solve the unsolvable history of the early twentieth century. Table 2 shows the details of stratigraphic layer, compressibility, initial thickness & depth.

9.2 Jakarta: The Coastal InSAR Revolution

Jakarta, Indonesia, faces a coastal crisis of unparalleled severity, with catastrophic localized maximum subsidence rates reaching 26 cm/year in northwestern coastal districts. To monitor this crisis and design the planned "Giant Sea Wall", the geotechnical community has aggressively adopted persistent scatterer interferometric synthetic aperture radar (PS-InSAR) satellite data. However, satellite geodesy suffers from a fundamental temporal limitation: it only captures the rate of geometric change during the specific operational lifespan of the satellite constellation. It

does not provide the historical settlement curve tracing back to the onset of the groundwater drawdown (t_0). Traditional calculus is incapable of predicting the ultimate consolidation limit of Jakarta's alluvial plains because the initial starting state is unrecorded. The X-Y-Y' framework bridges this critical gap flawlessly. By feeding massive datasets of instantaneous velocity (Rate,

Table 2: Mexico City subcrustal details

Stratigraphic Layer	Depth Range (m)	Compressibility (mv, 1/kPa)	Initial Thickness (m)
Artificial Fill	0.00 - 7.00	0.0003	7.00
Upper Clay Formation	7.00 - 23.00	0.0021	16.00
Middle Clay Formation	23.00 - 38.50	0.0010	15.50
Hard Draining Layer	38.50 - 41.00	0.0000	2.50
Lower Clay Formation	41.00 - 51.00	0.0006	10.00

Y') and current relative ground displacement (State, Y) provided by InSAR directly into the Y-Y' phase plane, engineers extract the macroscopic hydrodynamic Central Operator of the basin directly from the geometric slope of the satellite data points, allowing for precise future inundation forecasting.

9.3 Venice: The MOSE Project and Visco-Plastic Creep

To safeguard Venice, Italy, from the increasingly frequent and destructive high tides, the MOSE project required the installation of 78 massive mobile buoyancy flap gates on the seafloor of the lagoon.[1] The geotechnical design of the pivoting hinges for these gates was extraordinarily complex due to the highly heterogeneous stratigraphy, consisting of interbedded, highly variable layers of silty sands and over consolidated clays. In highly heterogeneous organic silts and peats, the boundary between primary fluid dissipation and secondary structural adjustment (creep) is

frequently blurred.

Traditional logarithmic time-fitting methods derived from Terzaghi's theory fail to accurately demarcate these overlapping phases, leading to dangerous underestimations of long-term settlement. The X-Y-Y' framework provides the optimal mathematical tool for analysing this specific data. By charting the precise vertical displacement data against the calculated velocity onto the Y-Y' plane, the distinct transition from primary hydrodynamic consolidation to secondary viscous creep becomes mathematically irrefutable. Primary consolidation forms a distinct linear slope on a standard linear Cartesian axis (Type I Linearity), while the secondary viscous creep transitions into a linear slope on a semi-logarithmic axis (Type IV Linearity). This clean geometric bifurcation allowed engineers to design the MOSE gate infrastructure to tolerate exact degrees of long-term differential settlement over its 50-year lifespan without the severe risk of the hinges binding during a storm surge.

9.4 The Leaning Tower of Pisa: A Forensic Masterpiece

The stabilization of the Leaning Tower of Pisa stands as the quintessential forensic geotechnical challenge of the modern era.[1] Construction began in 1173 and occurred in disjointed phases spanning 176 years. The inexorable, creeping increase in inclination over the subsequent eight centuries was driven primarily by the secondary consolidation (viscous creep) of the deep Pancone clay layer. If an investigating engineer attempts to determine the critical coefficient of secondary consolidation (α) using traditional classical equations, they encounter an immovable theoretical wall: the governing equations require the exact time of the load increment (t_0) to be definitively known. For a load applied dynamically and asymmetrically over 800 years ago, defining an exact t_0 is physically impossible.

Through the application of the X-Y-Y' calculus, this 800-year historical barrier is elegantly sidestepped. By defining the current State (the present degree of tilt, Y) and the current Rate (the exact velocity of the tilt, Y'), the current geometric trajectory of the tower is plotted securely in phase space. Because secondary consolidation represents a mathematically guaranteed linear trajectory on a semi-log Y-Y' plot (Type IV Linearity), the Central Operator—representing the exact physical creep characteristics of the underlying clay—is extracted directly from the slope of the recent historical data.[1] This purely geometric understanding provides the stabilization committee with the exact parameters required to design the highly successful under excavation technique, permanently stabilizing the tower all without ever needing to solve an explicit time-domain equation originating in the twelfth century.

10 Discussions: Visual Stability Diagnosis and Data Filtration

The transition from a restrictive time-centric perspective to a fluid phase-space perspective enables highly advanced visual stability diagnosis and automated data filtration. Field measurements of structural settlement are notoriously noisy and frequently exhibit overlapping,

complex multi-phase behavior. The δ-$log(d\delta/dt)$ diagnostic plot reveals the internal phase structure of the soil with remarkable clarity.

By projecting raw settlement data into this semi-logarithmic phase plane, up to seven distinct physical stages of deformation can be mathematically isolated and visually identified. Initial elastic compression manifests as a vertical drop (infinite velocity change). The first primary hydrodynamic consolidation (Type I) yields a distinct negatively sloped straight line representing strict Terzaghi behavior. Changes in drainage boundaries or structural stratigraphy manifest as curved inflection points (transition phases). Finally, true secondary consolidation (creep) is identified as a horizontal asymptotic approach or a shallower constant slope (Type IV).

This diagnostic capability facilitates sophisticated algorithmic data filtration techniques. Automated piecewise linear regression and Bayesian change-point detection algorithms can be deployed to systematically segment raw, noisy field data into these physically meaningful phases. By filtering out the noise and identifying the exact transition points, the framework ensures that the Central Operator is calculated exclusively from the valid linear segments of the trajectory. This protects the mathematical integrity of the parameter extraction process and produces a comprehensive quality metric, ensuring high confidence in predictive infrastructure modelling on a global scale.

11 Conclusions

The classical time-centric Newtonian calculus that has underpinned applied engineering mathematics since the seventeenth century is fundamentally incomplete when faced with the harsh, dissipative realities of modern forensic geotechnics and global infrastructure construction. Its strict mathematical reliance on known initial times (t_0), explicit temporal boundary conditions, and idealized homogeneous parameters renders it fragile, error-prone, and frequently entirely unusable when evaluating the long-term, non-linear consolidation of soils beneath critical megacity infrastructure.

The comprehensive three-dimensional X-Y-Y' framework successfully dismantles the mathematical tyranny of the temporal master variable. By elevating the observable State (Y) and the measurable Rate (Y') to the position of primary independent dimensions, the framework reveals the invariant, intrinsic geometric DNA of the soil consolidation process. Through the direct mathematical application of the three Asymptotic Linearity Theorems and the identification of the Central Operator, geotechnical engineers are now fully equipped to mathematically bypass the paralyzing Missing Time problem entirely. Time, within the strict context of dissipative physical deformation, is proven to be merely a dependent geometric consequence of the physical process.

By applying this advanced calculus to global infrastructure crises—from reconstructing the 800-year creep trajectory of the Leaning Tower of Pisa to interpreting massive arrays of raw InSAR

satellite velocity data to protect the subsiding coastal plains of Jakarta—the framework provides a level of predictive power, stability diagnosis, and historical reconstruction previously thought mathematically impossible.

12 Future Scope

The foundational principles of the X-Y-Y' phase plane analysis established in this paper provide a robust, highly adaptable platform for numerous advanced extensions in future research. The immediate scope involves the full mathematical integration of this framework into large-strain consolidation theories, where the magnitude of settlement is comparable to the overall layer thickness, thereby inducing significant geometric non-linearities. Furthermore, the framework's capacity to handle non-Darcy flow dynamics, prevalent in highly dense clays experiencing high hydraulic gradients, requires systematic evaluation.

Additionally, the expansion of the geometric superposition models to accommodate fully coupled thermo-hydro-mechanical (THM) processes will be crucial for the resilient design of energy geo-structures, nuclear waste repositories, and deep geothermal wellbore stability. Finally, the application of machine learning architectures—specifically physics-informed neural networks (PINNs)—to automate the real-time identification of the Central Operator from continuous autonomous sensor feeds represents a critical frontier. This will enable the rapid deployment of highly adaptive, real-time observational dashboards capable of instantly updating settlement predictions and structural safety factors across global megacities experiencing active seismic and subsidence threats.

13 Mandatory Declarations

Funding: The author declares that no funds, grants, or other financial support were received during the conceptualization, mathematical derivation, or preparation of this manuscript.

Conflict of Interest: None.

Ethical Approval: There are no human or animal participants involved in the conducted study.

Availability of Data and Material: All theoretical datasets, geometric iterations, mathematical derivations, and structural equations utilized to support the foundational conclusions of this study are comprehensively detailed and included within the body of the article itself. No proprietary or hidden datasets were utilized.

14 References

[1] Terzaghi, K., 1923, Mathematisch-naturewissenschaftliche Klasse, Akademie der Wissenschaften in Wien, Sitzungsberichte, Part Iia, Vol. 132, No. 3/4, pp.125-138.

[2] Casagrande, A., 1939, “Notes on Soil Testing for Engineering Purposes,” Soil Mech. Series No. 8, Publication from Graduate School of Engineering, No. 268, Howard University, Cambridge, Mass.

[3] D. W. Taylor, Fundamentals of Soil Mechanics. New York: John Wiley and Sons Inc., 1948.

[4] Parkin, A. K., 1978, "Coefficient of Consolidation by the Velocity Method," Geotechnique, Vol. 28, No. 4, pp. 472-474.

[5] R. E. Olson, "Consolidation under time-dependent loading," Journal of Geotechnical Engineering, vol. 103, no. 1, pp. 55-60, 1977.

[6] Biot, M. A., “General theory of three-dimensional consolidation,” Journal of Applied Physics, Vol. 12, No. 2, 1941, pp. 155–164.

[7] Carrillo, N., “Simple two- and three-dimension cases in the theory of consolidation of soils,” Journal of Mathematics and Physics, Vol. 21, No. 1, 1942, pp. 11–18.

[8] Barron, R. A., “Consolidation of Fine-Grained Soils by Drain wells,” Transactions of ASCE, Vol.113, 1948, pp. 718–724.

[9] Leo, C. J., “Equal Strain Consolidation by Vertical Drains,” ASCE Journal of Geotechnical and Geo-environmental Engineering, Vol. 130, No. 3, 2004, pp. 316–327.

[10] Tewatia, S. K., Evaluation of true *Cv* and instantaneous *Cv*, and isolation of secondary consolidation, ASTM Geotechnical Testing Journal, Vol. 21, No. 2, 1998, pp. 102–108.

[11] Tewatia, S. K., and Tewatia, K., Consolidation of Soils (book): Rate of Settlement Approach, 1st ed., Lambert Academic Publishing, 2019.

[12] Tewatia, S. K., Tewatia, K., and Tewatia, A., “Y-Y’ Calculus from Soil Consolidation to other Physical Sciences,” in Smart Geotechnics for Smart Societies, Taylor & Francis / CRC Press, 2023, pp. 88–105.